Thermophysical Properties of Solutions of Iron(III)nitrate-Nonahydrate in Mixtures of Ethanol and Water

Alexander Keller[1], Irenäus Wlokas[2], Maximilian Kohns*,[1], Hans Hasse[1]

[1]*University of Kaiserslautern, Laboratory of Engineering Thermodynamics, Erwin-Schrödinger-Str. 44, D-67663 Kaiserslautern, Germany*
[2]*University Duisburg-Essen, Fluid Dynamics, Institute for Combustion and Gas Dynamics, Carl-Benz-Str. 199, D-47057 Duisburg, Germany*

Abstract

The quality of nanoparticles that are obtained by spray flame synthesis depends strongly on the thermophysical properties of the precursor solutions. Solutions of iron(III)nitrate-nonahydrate (INN) in ethanol are interesting precursor solutions for the production of iron oxide nanoparticles in these processes. However, no data on thermophysical properties of solutions of INN in ethanol are available in the literature. Therefore, in the present work, the specific density, viscosity, thermal conductivity and molar isobaric heat capacity of solutions of INN in solvent mixtures of ethanol and water were measured at 101.3 kPa between 288.15 and 333.15 K, solvent compositions ranging from pure ethanol to pure water, and INN molalities up to 1.3 mol kg^{-1}. Empirical correlations of the experimental data are provided.

* Corresponding author; maximilian.kohns@mv.uni-kl.de

1. Introduction

Spray flame synthesis is an interesting process for the production of nanoparticles. In that process, the pyrolysis of aerosol droplets of a combustible precursor solution leads to the formation of nanoparticles. Different combinations of metal-containing substances and combustible solvents have been used to obtain various forms of nanoparticles[1–4]. For gaining insight into the phenomena in the spray flame and for the design and optimization of the process, simulations are performed, for which information on the thermophysical properties of the precursor solutions[5–7] is needed, namely the density, viscosity, thermal conductivity and isobaric heat capacity. In a recent work of our group, these properties were investigated for precursor solutions for the production of titanium oxide nanoparticles[8]. A further motivation to investigate thermophysical properties of precursor solutions is the recent suggestion of a standardized synthesis setup by the SpraySyn initiative[9], in which also benchmark precursor systems were defined.

Iron(III)nitrate-nonahydrate ($Fe(NO_3)_3 \cdot 9\ H_2O$, INN) is a common precursor used in spray flame synthesis processes for the production of iron oxide nanoparticles [1–3,9–14]. A popular solvent for INN is ethanol[2,9,12–15]. As INN releases its nine crystal water molecules upon dissolution in ethanol, precursor solutions of INN in ethanol always contain large amounts of water. Recently, Stodt et al.[15] investigated the chemistry of INN-based precursor-solutions for the spray flame synthesis process, such as INN + ethanol, with Fourier-transform infrared spectroscopy. As ethanol has a higher vapor pressure than water, and water has a strong affinity to the ions, ethanol will evaporate from the precursor solution droplet preferentially, leading to an increase of the water concentration in the droplet. Hence, for the simulation of the evaporation process, not

only the thermophysical properties of solutions of INN in pure ethanol are required but also those of INN in ethanol with additional water. Moreover, water produced by combustion in the flame may enter the droplet by mass transfer from the gas phase[13].

Despite the high interest in the spray flame synthesis of nanoparticles from INN solutions, thermophysical data are only available for the pure solvents and the salt-free solvent mixture of ethanol and water, but are scarce for solutions of INN. There are only two papers in the literature that report the density of aqueous solutions of INN[16,17]. To the best of our knowledge, no information is available on ethanolic INN solutions.

In contrast, abundant data are available in the literature for mixtures of ethanol and water (without INN). Many authors have measured their density[18–30]. The molar excess volume of these mixtures is negative, which is attributed to H-bonding and the resulting structuring of the ethanol + water solutions. Also the mixture viscosity has been reported by several authors[18–21,31–33]. The viscosity of mixtures of ethanol and water is higher than that of the pure components, which is again attributed to the H-bonding between the molecules. Several authors[34–38] measured the thermal conductivity of mixtures of ethanol and water. For pure ethanol, the thermal conductivity decreases with increasing temperature. For pure water, the trend is opposite. As a result, mixture compositions can be found for which the temperature dependence of the thermal conductivity changes its sign[37]. The isobaric heat capacity of mixtures of ethanol and water was measured by two groups[39,40] and a positive excess was found.

To summarize: the properties of mixtures of ethanol and water are well-known. In contrast, not much is known about the properties of solutions of INN in these

solvents, only the specific density of aqueous INN solutions has been reported in the literature. Thus, the specific density, viscosity, thermal conductivity and molar isobaric heat capacity in solutions of INN in mixtures of ethanol and water were measured in the present work at the temperature range from 288.15 to 333.15 K and ambient pressure, with solvent compositions ranging from pure ethanol to pure water and overall INN molalities up to 1.3 mol kg^{-1}. Empirical correlations of the data were established, which facilitate the application of the new information on the thermophysical properties in numerical simulations.

For the sake of brevity, we write "density" for "specific density" and "isobaric heat capacity" for "molar isobaric heat capacity". The specified standard uncertainties for all measurements include statistical and method uncertainties.

2. Experimental

2.1 Chemicals and sample preparation

INN and ethanol were purchased from Sigma-Aldrich and used without further purification. Information on the CAS registry number and purity are listed in Table 1.

[Table 1 about here.]

Water from a Milli-Q System (Millipore) with a specific electrical resistance greater than 18.2 MΩcm was used for preparing the aqueous solutions. INN was handled in a nitrogen atmosphere in an inert gas glove box (GS Glovebox Technik), with a water content below $2 \cdot 10^{-6}$ g g^{-1} and an oxygen content below $1.2 \cdot 10^{-6}$ g g^{-1}. Samples were prepared using a laboratory balance (Mettler-Toledo AG204) with a standard uncertainty of $u(m) = 0.0001$ g.

2.2 Measurements

All measurements of solutions of INN in ethanol, INN in water, or INN in mixtures of ethanol and water were performed at $p = 101.3$ kPa, with a standard uncertainty of $u(p) = 3$ kPa. Throughout this article, the mixtures are considered as ternary systems comprising the components INN ($Fe(NO_3)_3 \cdot 9\ H_2O$), ethanol and water, i.e. the overall composition of the solution is reported. Salt-free properties are denoted by a circumflex (^). The composition of the ternary mixtures is specified by the overall molality of INN b_{INN} and the mole fraction of ethanol (E) in the salt-free solvent mixture $\hat{x}_E$, which are defined as follows. The overall molality b_{INN} is

$$b_{INN} = \frac{n_{INN}}{\hat{m}_{Solv}} \ . \tag{1}$$

Here, n_{INN} is the number of moles of INN and $\hat{m}_{Solv}$ is the mass of the INN-free solvent mixture

$$\hat{m}_{Solv} = n_E \cdot M_E + n_W \cdot M_W \ , \tag{2}$$

where n_E and n_W denote the mole numbers of the solvents ethanol and water (W), respectively. The mole fraction of ethanol in the salt-free solvent mixture $\hat{x}_E$ is given by

$$\hat{x}_E = \frac{n_E}{n_E + n_W} \ . \tag{3}$$

In the experiments carried out in the present work, the overall INN molality varied between $0 \leq b_{INN} \leq 1.3$ mol kg^{-1}, and the solvent composition varied between $0 \leq \hat{x}_E \leq 1$ mol mol^{-1}. From an error propagation of the steps in the gravimetrical sample preparation, the standard uncertainty of b_{INN} is estimated to be $u(b_{INN}) = 0.005$ mol kg^{-1} and the standard uncertainty of $\hat{x}_E$ is estimated to be

$u(\hat{x}_E) = 0.0005$ mol mol^{-1}. All samples were hermetically sealed in 40 mL glass vials and measurements were performed within 1 h after sample preparation.

2.2.1 Density and shear viscosity

The measurements of the liquid density and viscosity were carried out using an instrument of Anton Paar (SVM 3000) at 293.15 to 333.15 K. The density measurements were conducted with the vibrating tube technique according to the ASTM method D4052, with a relative standard uncertainty $u_r(\rho) = 0.002$, and the viscosity measurements were conducted with a Stabinger viscosimeter according to the ASTM method D7042 with a relative standard uncertainty ranging from $u_r(\eta) = 0.02$ (for pure ethanol as the solvent) to $u_r(\eta) = 0.07$ (for pure water as the solvent). The increase of the relative standard uncertainty in the viscosity for mixtures with high water contents results from an incomplete wetting of the Stabinger viscosimeter by the samples. After each set of measurements, the apparatus was cleaned twice with water and ethanol and flushed with dry air. The temperature was measured with a built-in thermometer, for which the manufacturer claims a standard uncertainty of $u(T) = 0.05$ K. The apparatus was calibrated with calibration standards provided by the manufacturer. For validation, the density and viscosity of ethanol + water were measured and compared to literature values of several authors. Additionally, the density data of solutions of INN in water at 298.15 K of Arrad et al.[16] were compared to the data of this work. The results of these comparisons are presented in the Supporting Information. Heydweiller[17] also reports data for the density of such solutions, however, the employed measure of concentration is not defined clearly in his work, so that a comparison with the present data is not possible. The relative deviations d_r between the reported density data and the own

measurements are $d_r(\rho) \leq 0.0016$. Relative deviations between the reported viscosity data are $d_r(\eta) \leq 0.02$ for pure ethanol and $d_r(\eta) \leq 0.05$ for mixtures of ethanol and water.

2.2.2 *Thermal conductivity and isobaric heat capacity*

The measurements of the thermal conductivity and the isobaric heat capacity were carried out with an instrument of flucon fluid control GmbH (LAMBDA) at 288.15, 298.15 and 308.15 K. In the instrument, the transient hot wire method according to the ASTM method D7896 was applied to determine the thermal conductivity λ and the thermal diffusivity a. The molar isobaric heat capacity c_p was then calculated by the relationship

$$c_p = \frac{\lambda \cdot \overline{M}}{a \cdot \rho} \quad ,$$

(4)

where the specific density ρ of the liquid was determined as explained in the previous section. The reported values of λ and c_p are the average over 10 measurements. The relative standard uncertainty of the thermal conductivity measurement is estimated to be $u_r(\lambda) = 0.03$, and the relative standard uncertainty of the isobaric heat capacity measurement is estimated to be $u_r(c_p) = 0.05$ for INN in the pure solvents and $u_r(c_p) = 0.1$ for INN in mixtures of ethanol and water. After each set of measurements, the apparatus was cleaned with water and ethanol and flushed with dry air. The sensor and sample are thermostatted by a double jacket vessel, in which preheated water is circulating. The temperature was measured with a built-in Pt100 resistance thermometer. The standard uncertainty of the temperature measurement is $u(T) = 0.2$ K. For the measurement of the thermal conductivity, the apparatus was calibrated to the thermal conductivities of pure ethanol and pure water at 293.15 K. For the measurement of the isobaric heat capacity, the apparatus was

calibrated to the isobaric heat capacities of pure ethanol and pure water at 293.15 K. For validation, the thermal conductivity and isobaric heat capacity of mixtures of ethanol and water were measured and compared to literature values of several authors. The results are presented in the Supporting Information. The relative deviations between the reported thermal conductivity data and our own measurements are $d_r(\lambda) \leq 0.025$ for pure ethanol, $d_r(\lambda) \leq 0.02$ for pure water, and $d_r(\lambda) \leq 0.03$ for mixtures of ethanol and water. The relative deviations between the reported isobaric heat capacity data are $d_r(c_p) \leq 0.03$ for pure ethanol and $d_r(c_p) \leq 0.005$ for pure water.

3. Modeling

For correlating the specific density ρ, the values are converted to molar volumes v,

$$v = \frac{\bar{M}}{\rho} \quad .$$ (5)

where $\bar{M}$ is the mean molar mass of the mixture consisting of solvent ethanol, solvent water and INN (the INN crystal water does not add on to the solvent water). The molar volume of a mixture is represented as a sum of two terms:

$$v = v_{Solv} + \xi$$ (6)

The first term, v_{Solv}, is the molar volume of the INN-free solvent mixture. The second term, ξ, accounts for the influence of INN on the molar volume. Both terms are correlated here by simple polynomials in composition and temperature. The molar volume of the INN-free solvent mixture v_{Solv} is described by

$$v_{Solv} = \hat{x}_E v_E^{pure} + \hat{x}_W v_W^{pure} + v_{Solv}^E \quad .$$ (7)

Here, v_E^{pure} and v_W^{pure} are the temperature-dependent pure component molar volumes of ethanol and water,

$$v^{\text{pure}} / \text{cm}^3\text{mol}^{-1} = a + b \cdot (T / K) + c \cdot (T / K)^2 \ , \tag{8}$$

where a, b and c are adjustable parameters.

The excess molar volume $v_{\text{Solv}}^{\text{E}}$ of the solvent mixture is correlated using a Redlich-Kister polynomial,

$$\frac{v_{\text{Solv}}^{\text{E}}}{\text{cm}^3\text{mol}^{-1}} = A \cdot \hat{x}_{\text{E}} \hat{x}_{\text{W}}$$
$$+ B \cdot \hat{x}_{\text{E}} \hat{x}_{\text{W}} \cdot (\hat{x}_{\text{E}} - \hat{x}_{\text{W}}) \ , \tag{9}$$
$$+ C \cdot \hat{x}_{\text{E}} \hat{x}_{\text{W}} \cdot (\hat{x}_{\text{E}} - \hat{x}_{\text{W}})^2$$

where A, B and C are temperature-dependent adjustable parameters, which are correlated with

$$A = d + e \cdot (T / K) + f \cdot (T / K)^2 \ . \tag{10}$$

The term ξ, which describes the influence of INN on the molar volume, is given by

$$\xi / \text{cm}^3\text{mol}^{-1} = x_{\text{INN}} \cdot \left(D + E \cdot \hat{x}_{\text{E}} + F \cdot \hat{x}_{\text{E}}^2 + G \cdot \hat{x}_{\text{E}}^3 \right)$$
$$+ x_{\text{INN}}^2 \cdot \left(H + I \cdot \hat{x}_{\text{E}} + J \cdot \hat{x}_{\text{E}}^2 + K \cdot \hat{x}_{\text{E}}^3 \right) \ . \tag{11}$$

Here, x_{INN} is the mole fraction of INN in the mixture, and D, E, F, G, H, I, J and K are temperature-dependent adjustable parameters, which are correlated with

$$D = g + h \cdot (T / K) \ . \tag{12}$$

The mole fraction of INN in the mixture x_{INN} is defined as

$$x_{\text{INN}} = \frac{n_{\text{INN}}}{n_{\text{INN}} + n_{\text{E}} + n_{\text{W}}} \ , \tag{13}$$

where n_{INN}, n_{E} and n_{W} are the mole numbers of INN, ethanol and water, respectively. Inserting Eq. (13) in Eq. (1) and rearranging leads to the conversion of b_{INN} to x_{INN} as follows

$$x_{INN} = \frac{b_{INN}}{b_{INN} + \dfrac{1}{\overline{M}_{Solv}}} \cdot \qquad (14)$$

Here, $\overline{M}_{Solv}$ is the mean molar mass of the salt-free solvent mixture.

The viscosity η (in units mPa s), thermal conductivity λ (in units mW m^{-1}K^{-1}) and isobaric heat capacity c_p (in units J mol^{-1}K^{-1}) are correlated in the same way as the molar volume, i.e. using Eqs. (6) - (14).

In most cases, not all of the polynomial coefficients in Eqs. (8) - (12) are needed. Only those terms required for obtaining a satisfactory fit of the data were included to reduce the risk of overfitting and to allow meaningful extrapolations of the correlations to some extent. Also other approaches to correlating the data were tested, e.g. using the INN molality b_{INN} instead of the INN mole fraction x_{INN}, but necessitated the use of more adjustable parameters.

In order to obtain an adequate fit of the experimental data, parameters were adjusted using a least squares minimization performed by the MATLAB®[41] solver "lsqnonlin", using the objective function

$$OF = \sum_{i=1}^{N_p} \left(\frac{z_i^{exp} - z_i^{cal}}{z_i^{exp}} \right)^2 , \qquad (15)$$

where z is either of the properties considered in this work and N_p is the number of experimental points. The superscripts "exp" and "cal" denote experimental and calculated results.

4. Results and discussion

In the following sections, results for the different properties of mixtures of INN, ethanol and water are shown as functions of the mole fraction of ethanol in the INN-

free solvent mixture $\hat{x}_E$, the overall molality b_{INN} and temperature T. The experimental data are reported in Tables 2 – 5 and repeated for convenience in the Supporting Information as a function of the true mole fractions in the mixture. The correlation parameters, cf. Eqs. (8) - (12), are provided in Tables 6 - 8. Results for the thermal diffusivity a are shown in the Supporting Information.

4.1 Density

The experimental data of the density of solutions of INN in mixtures of ethanol and water obtained in the present work are shown in Figure 1 together with the correlation.

[Figure 1 about here.]

The density increases with increasing molality of INN and with decreasing temperature. For b_{INN} = 0.74 mol kg^{-1} and T = 333.15 K in pure ethanol the precipitation of a solid was observed after sample preparation, which is the reason for the missing data point. Astonishingly, no precipitation was observed for higher or lower overall molalities of INN or lower temperatures. Studying the solid precipitation in mixtures of INN and ethanol is beyond the scope of the present work. The correlation describes the experimental data within the experimental standard uncertainty.

4.2 Viscosity

The experimental data of the viscosity of solutions of INN in mixtures of ethanol and water obtained in the present work are shown in Figure 2 together with the correlation.

[Figure 2 about here.]

The viscosity of mixtures of INN and ethanol increases with increasing molality of INN and with decreasing temperature. The same holds for aqueous solutions and mixed solvents. As for the density, no experimental data for $b_{INN} = 0.74$ mol kg^{-1} and $T = 333.15$ K in pure ethanol can be reported here due to the formation of a solid precipitate. Due to the incomplete wetting of the Stabinger viscosimeter mentioned above, data on the viscosity of pure water used for establishing the correlation were taken from the literature[42–45]. The correlation describes the experimental data within the experimental standard uncertainty, except for high INN molalities and low temperatures, where the slope of the viscosity is steep.

4.3 Thermal conductivity

The experimental data of the thermal conductivity of solutions of INN in mixtures of ethanol and water obtained in the present work are shown in Figure 3 together with the correlation. As we have only considered one composition of the salt-free solvent mixture, additional data of the thermal conductivity of mixtures of ethanol and water were taken from the literature[34–37] for establishing the correlation.

[Figure 3 about here.]

The dependence of the thermal conductivity of mixtures of INN, ethanol and water on the variables T, $\hat{x}_E$, and b_{INN} is more complex than for the other properties studied here. There are several interesting features: Firstly, for pure ethanol as the solvent an invariant point is observed, in which all isotherms $\lambda(b_{INN})$ intersect at $b_{INN} = 0.12$ mol kg^{-1}. This is due to the fact that the temperature dependence of λ is different for pure water, for which λ increases with T, and pure ethanol, for which the opposite trend is observed. Thus, the invariant point observed for pure ethanol as the solvent arises from the fact that adding INN also means adding water. A similar

invariant point is also observed for the salt-free solvent mixture[37]. Secondly, depending on the composition of the solvent, the curves $\lambda(b_{INN})$ show maxima or minima. For pure water as the solvent minima are observed at all temperatures, for pure ethanol as the solvent maxima are observed instead. For the intermediate $\hat{x}_E = 0.28$ mol mol^{-1} the curves $\lambda(b_{INN})$ are flat for all studied temperatures. We have explored plotting the results for λ as a function of the true mole fractions but have not found simpler trends. The correlation describes the experimental data within the experimental standard uncertainty.

4.4 Isobaric heat capacity

The experimental data of the isobaric heat capacity of solutions of INN in mixtures of ethanol and water obtained in the present work are shown in Figure 4 together with the correlation. Due to the high deviation to the literature data[39,40] of the heat capacity measurements of the mixtures of ethanol and water, experimental data for the excess heat capacity for the salt-free solvent mixture $c_{p,Solv}^E$ were taken from the literature[39,40] for establishing the correlation.

[Figure 4 about here.]

The isobaric heat capacity of mixtures of INN, ethanol and water decreases with increasing molality of INN and with increasing temperature. The correlation describes the experimental data within the experimental standard uncertainty.

5. Conclusions

In the present work, thermophysical properties of mixtures of iron(III)nitrate-nonahydrate (INN), ethanol and water, which are used in spray flame synthesis processes for the production of iron oxide nanoparticles, were measured. The

presented data include the density, viscosity, thermal conductivity and isobaric heat capacity. From this comprehensive set of data, only the density of the binary system INN + water was available previously. Empirical correlations to the thermophysical data are provided. The data presented here establish a basis for the simulation of spray flame synthesis processes for the production of iron oxide nanoparticles and can thereby contribute to a better understanding of the droplet atomization and evaporation process of the precursor solution.

6. Acknowledgements

7. Associated content

Supporting Information Available: Comparison of experimental data for pure ethanol, pure water, mixtures of ethanol and water, and densities of aqueous solutions of INN to literature data; results for the thermal diffusivity, experimental results as functions of the true mole fractions.

References

(1) Teoh, W. Y.; Amal, R.; Mädler, L. Flame Spray Pyrolysis : An Enabling Technology for Nanoparticles Design and Fabrication. *Nanoscale* **2010**, *2*, 1324–1347.

(2) Strobel, R.; Pratsinis, S. E. Direct Synthesis of Maghemite, Magnetite and Wustite Nanoparticles by Flame Spray Pyrolysis. *Adv. Powder Technol.* **2009**, *20*, 190–194.

(3)   Morales, M. P.; González-Carreño, T.; Ocaña, M.; Alonso-Sañudo, M.; Serna, C. J. Magnetic Iron Oxide/Mullite Nanocomposite Stable up to 1400°C. *J. Solid State Chem.* **2000**, *155*, 458–462.

(4)   Grimm, S.; Schultz, M.; Barth, S.; Müller, R. Flame Pyrolysis – a Preparation Route for Ultrafine Pure γ-Fe2O3 Powders and the Control of Their Particle Size and Properties. *J. Mater. Sci.* **1997**, *32*, 1083–1092.

(5)   Sirignano, W. A. *Fluid Dynamics and Transport of Droplets and Sprays*; Cambridge University Press, 1999.

(6)   Rittler, A.; Deng, L.; Wlokas, I.; Kempf, A. M. Large Eddy Simulations of Nanoparticle Synthesis from Flame Spray Pyrolysis. *Proc. Combust. Inst.* **2017**, *36*, 1077–1087.

(7)   Abramzon, B.; Sirignano, W. A. Droplet Vaporization Model for Spray Combustion Calculations. *Int. J. Heat Mass Transf.* **1989**, *32*, 1605–1618.

(8)   Keller, A.; Wlokas, I.; Kohns, M.; Hasse, H. Thermophysical Properties of Mixtures of Titanium(IV) Isopropoxide (TTIP) and p-Xylene. *J. Chem. Eng. Data* **2020**, *65*, 869–876.

(9)   Schneider, F.; Suleiman, S.; Menser, J.; Borukhovich, E.; Wlokas, I.; Kempf, A.; Wiggers, H.; Schulz, C. SpraySyn—A Standardized Burner Configuration for Nanoparticle Synthesis in Spray Flames. *Rev. Sci. Instrum.* **2019**, *90*, 085108.

(10)   González-Carreño, T.; Morales, M. P.; Gracia, M.; Serna, C. J. Preparation of Uniform γ-Fe2O3 Particles with Nanometer Size by Spray Pyrolysis. *Mater. Lett.* **1993**, *18*, 151–155.

(11) Cabañas, M. V.; Vallet-Regí, M.; Labeau, M.; González-Calbet, J. M. Spherical Iron Oxide Particles Synthesized by an Aerosol Technique. *J. Mater. Res.* **1993**, *8*, 2694–2701.

(12) Dosev, D.; Nichkova, M.; Dumas, R. K.; Gee, S. J.; Hammock, B. D.; Liu, K.; Kennedy, I. M. Magnetic/Luminescent Core/Shell Particles Synthesized by Spray Pyrolysis and Their Application in Immunoassays with Internal Standard. *Nanotechnology* **2007**, *18*, 055102.

(13) Rosebrock, C. D.; Wriedt, T.; Mädler, L.; Wegner, K. The Role of Microexplosions in Flame Spray Synthesis for Homogeneous Nanopowders from Low-Cost Metal Precursors. *AIChE J.* **2016**, *62*, 381–391.

(14) Strobel, R.; E. Pratsinis, S. Effect of Solvent Composition on Oxide Morphology during Flame Spray Pyrolysis of Metal Nitrates. *Phys. Chem. Chem. Phys.* **2011**, *13*, 9246–9252.

(15) Stodt, M. F. B.; Gonchikzhapov, M.; Kasper, T.; Fritsching, U.; Kiefer, J. Chemistry of Iron Nitrate-Based Precursor Solutions for Spray-Flame Synthesis. *Phys. Chem. Chem. Phys.* **2019**, *21*, 24793–24801.

(16) Arrad, M.; Kaddami, M.; Sippola, H.; Taskinen, P. Thermodynamic Modeling of Apparent Molal Volumes of Metal Nitrate Salts with Pitzer Model. *J. Chem. Eng. Data* **2015**, *60*, 856–859.

(17) Heydweiller, A. Elektrische Leitfähigkeit Und Dichte Wäßriger Elektrolytlösungen. *Z. Für Anorg. Allg. Chem.* **1921**, *116*, 42–44.

(18) Pires, R. M.; Costa, H. F.; Ferreira, A. G. M.; Fonseca, I. M. A. Viscosity and Density of Water + Ethyl Acetate + Ethanol Mixtures at 298.15 and 318.15 K and Atmospheric Pressure. *J. Chem. Eng. Data* **2007**, *52*, 1240–1245.

(19) Khattab, I. S.; Bandarkar, F.; Fakhree, M. A. A.; Jouyban, A. Density, Viscosity, and Surface Tension of Water+ethanol Mixtures from 293 to 323K. *Korean J. Chem. Eng.* **2012**, *29*, 812–817.

(20) D'Aprano, A.; Fuoss, R. M. Electrolyte-Solvent Interaction. XX. Picric Acid in Mixtures of Acetonitrile and Basic Solvents. *J. Phys. Chem.* **1969**, *73*, 400–406.

(21) Ernst, R. C.; Watkins, C. H.; Ruwe, H. H. The Physical Properties of the Ternary System Ethyl Alcohol–Glycerin–Water. *J. Phys. Chem.* **1936**, *40*, 627–635.

(22) Atik, Z. Densities and Excess Molar Volumes of Binary and Ternary Mixtures of Aqueous Solutions of 2,2,2-Trifluoroethanol with Acetone and Alcohols at the Temperature of 298.15 K and Pressure of 101 KPa. *J. Solut. Chem.* **2004**, *33*, 1447–1466.

(23) Porcedda, S.; Leo, M.; Usula, M.; Piras, A. Excess Enthalpies and Excess Volumes of Binary Mixtures Containing a Linear Carboxylic Acid + Di-Iso-Propyl Ether at 298.15 K and 0.1 MPa. *J. Therm. Anal. Calorim.* **2016**, *125*, 607–615.

(24) Shalmashi, A.; Amani, F. Densities and Excess Molar Volumes for Binary Solution of Water+ Ethanol,+ Methanol And+ Propanol from (283.15 TO 313.15) K. *Lat. Am. Appl. Res.* **2014**, *44*, 163–166.

(25) Safarov, D. T.; Shakhverdiev, A. N. Investigation of the Thermophysical Properties of Ethyl Alcohol + Water Solutions. *High Temp.* **2001**, *39*, 395–400.

(26) Ivanov, E. V. Volumetric Properties of Dilute Solutions of Water in Ethanol and Water-D2 in Ethanol-D1 between T=(278.15 and 318.15)K. *J. Chem. Thermodyn.* **2012**, *47*, 162–170.

(27) Zhang, R.; Yan, W.; Wang, X.; Lin, R. Molar Excess Enthalpies of Ethyl Acetate+alkanols at T=298.15K, P=10.0MPa. *Thermochim. Acta* **2005**, *429*, 155–161.

(28) Pečar, D.; Doleček, V. Volumetric Properties of Ethanol–Water Mixtures under High Temperatures and Pressures. *Fluid Phase Equilibria* **2005**, *230*, 36–44.

(29) Takiguchi, Y.; Osada, O.; Uematsu, M. Thermodynamic Properties of {xC2H5OH+(1−x)H2O} in the Temperature Range from 320 K to 420 K at Pressures up to 200 MPa. *J. Chem. Thermodyn.* **1996**, *28*, 1375–1385.

(30) Arce, A.; Martínez-Ageitos, J.; Mendoza, J.; Soto, A. Water + Ethanol + 2-Methoxy-2-Methylbutane: Properties of Mixing at 298.15 K and Isobaric Vapour-Liquid Equilibria at 101.32 KPa. *Fluid Phase Equilibria* **1997**, *141*, 207–220.

(31) Whorton, R.; Edward, S. A. The Equivalent Conductance of Electrolytes in Mixed Solvents. *Z. Für Phys. Chem.* **2011**, *17*, 300–314.

(32) Bruun, S. G.; Graae Soerensen, P.; Hvidt, A. Ultrasonic Properties of Ethanol-Water Mixtures. *Acta Chem Scand A* **1974**, *28*, 1047–1054.

(33) Motin, M. A.; Kabir, M. H.; Huque, M. E. Viscosities and Excess Viscosities of Methanol, Ethanol and n-Propanol in Pure Water and in Water + Surf Excel Solutions at Different Temperatures. *Phys. Chem. Liq.* **2005**, *43*, 123–137.

(34) Assael, M. J.; Charitidou, E.; Wakeham, W. A. Absolute Measurements of the Thermal Conductivity of Mixtures of Alcohols with Water. *Int. J. Thermophys.* **1989**, *10*, 793–803.

(35) Qun-Fang, L.; Rui-Sen, L.; Dan-Yan, N.; Yu-Chun, H. Thermal Conductivities of Some Organic Solvents and Their Binary Mixtures. *J. Chem. Eng. Data* **1997**, *42*, 971–974.

(36) Wang, J.; Fiebig, M. Measurement of the Thermal Diffusivity of Aqueous Solutions of Alcohols by a Laser-Induced Thermal Grating Technique. *Int. J. Thermophys.* **1995**, *16*, 1353–1361.

(37) Zhou, J.-C.; Che, Y.-Y.; Wu, K.-J.; Shen, J.; He, C.-H. Thermal Conductivity of DMSO + C_2H_5OH, DMSO + H_2O, and DMSO + C_2H_5OH + H_2O Mixtures at T = (278.15 to 338.15) K. *J. Chem. Eng. Data* **2013**, *58*, 663–670.

(38) Gillam, D. G.; Lamm, O. Precision Measurements of the Thermal Conductivities of Certain Liquids Using the Hot Wire Method. *Acta Chem. Scand.* **1955**, *9*, 657–660.

(39) Grolier, J.-P. E.; Wilhelm, E. Excess Volumes and Excess Heat Capacities of Water + Ethanol at 298.15 K. *Fluid Phase Equilibria* **1981**, *6*, 283–287.

(40) Benson, G. C.; D'Arcy, P. J. Excess Isobaric Heat Capacities of Water-n-Alcohol Mixtures. *J. Chem. Eng. Data* **1982**, *27*, 439–442.

(41) *MATLAB R2014b*; The Mathworks, Inc.: Natick, Massachusetts, US.

(42) Abu-Daabes, M. A.; Awwad, A. M. Volumetric and Viscometric Properties of Aqueous Solutions of N-(2-Hydroxyethyl)Morpholine at T=(293.15, 303.15, 313.15, 323.15, 333.15)K. *J. Chem. Thermodyn.* **2008**, *40*, 874–878.

(43) Alam, Md. S.; Ashokkumar, B.; Mohammed Siddiq, A. The Density, Dynamic Viscosity and Kinematic Viscosity of Protic Polar Solvents (Pure and Mixed Systems) Studies: A Theoretical Insight of Thermophysical Properties. *J. Mol. Liq.* **2018**, *251*, 458–469.

(44) Gong, Y.; Shen, C.; Lu, Y.; Meng, H.; Li, C. Viscosity and Density Measurements for Six Binary Mixtures of Water (Methanol or Ethanol) with an Ionic Liquid ([BMIM][DMP] or [EMIM][DMP]) at Atmospheric Pressure in the Temperature Range of (293.15 to 333.15) K. *J. Chem. Eng. Data* **2012**, *57*, 33–39.

(45) Li, X.-X.; Zhang, M.; Wu, X.-X.; Wang, Y.-W.; Fan, G.-C.; Ma, X.-X. Thermodynamic and Spectroscopic Studies for Aqueous Solution of Ethylene Glycol Monomethyl Ether. *J. Mol. Liq.* **2011**, *158*, 92–96.

Table 1: Chemical specification.

	CAS reg. no.	supplier	Purity	analysis method
$Fe(NO_3)_3 \cdot 9\,H_2O$	7782-61-8	Sigma Aldrich	$\geq 0,9995$ g g^{-1}	-
C_2H_5OH	64-17-5	Sigma Aldrich	$\geq 0,9999$ g g^{-1}	^{1}H-NMR spectroscopy

Table 2: Results of the density measurements: ethanol mole fraction of the INN-free solvent mixture $\hat{x}_E$, overall INN molality b_{INN}, temperature T, density ρ. The pressure is 101.3 kPa. The standard uncertainties are $u(\hat{x}_E) = 0.0005$ mol mol^{-1}, $u(b_{INN}) = 0.005$ mol kg^{-1}, $u(T) = 0.05$ K, $u_r(\rho) = 0.002$ and $u(p) = 3$ kPa.

$\hat{x}_E$	b_{INN}	ρ / g cm^{-3}				
mol mol^{-1}	mol kg^{-1}	$T = 293.15$	303.15 K	313.15 K	323.15 K	333.15 K
0	0	0.9984	0.9957	0.9923	0.9880	0.9831
	0.248	1.0414	1.0382	1.0343	1.0298	1.0244
	0.495	1.0804	1.0764	1.0719	1.0671	1.0617
	0.743	1.1154	1.1112	1.1064	1.1009	1.0955
	0.990	1.1462	1.1417	1.1365	1.1311	1.1254
	1.237	1.1752	1.1702	1.1648	1.1590	1.1529
0.1153	0	0.9622	0.9566	0.9503	0.9434	0.9363
	0.248	1.0036	0.9982	0.9919	0.9853	0.9784
	0.495	1.0417	1.0359	1.0294	1.0227	1.0156
	0.743	1.0758	1.0699	1.0634	1.0568	1.0499
	0.990	1.1070	1.1008	1.0942	1.0873	1.0801
	1.238	1.1346	1.1284	1.1218	1.1149	1.1079
0.2811	0	0.9144	0.9042	0.8965	0.8892	0.8803
	0.248	0.9577	0.9497	0.9415	0.9330	0.9245
	0.495	0.9963	0.9885	0.9804	0.9720	0.9636
	0.742	1.0314	1.0236	1.0155	1.0071	0.9989
	0.990	1.0623	1.0546	1.0466	1.0385	1.0302
	1.237	1.0916	1.0838	1.0758	1.0676	1.0592
0.5399	0	0.8561	0.8474	0.8384	0.8293	0.8198
	0.248	0.9009	0.8924	0.8835	0.8745	0.8655
	0.495	0.9423	0.9337	0.9248	0.9157	0.9063
	0.743	0.9781	0.9694	0.9606	0.9515	0.9421
	0.990	1.0121	1.0036	0.9950	0.9859	0.9765
	1.238	1.0426	1.0339	1.0249	1.0157	1.0063
1	0	0.7898	0.7812	0.7724	0.7634	0.7541
	0.247	0.8367	0.8278	0.8186	0.8089	0.7988
	0.495	0.8793	0.8702	0.8607	0.8510	0.8400
	0.743	0.9183	0.9089	0.8994	0.8896	n.a.
	0.990	0.9538	0.9443	0.9345	0.9245	0.9144
	1.238	0.9887	0.9789	0.9689	0.9586	0.9479

Table 3: Results of the viscosity measurements: ethanol mole fraction of the INN-free solvent mixture $\hat{x}_E$, overall INN molality b_{INN}, temperature T, viscosity η. The pressure is 101.3 kPa. The standard uncertainties are $u(\hat{x}_E) = 0.0005$ mol mol^{-1}, $u(b_{INN}) = 0.005$ mol kg^{-1}, $u(T) = 0.05$ K and $u(p) = 3$ kPa. The relative standard uncertainties of the viscosity are given in the table.

$\hat{x}_E$ mol mol^{-1}	b_{INN} mol kg^{-1}	η / mPa s $T = 293.15$	303.15 K	313.15 K	323.15 K	333.15 K	$u_r(\eta)$
0	0.248	1.1935	0.9350	0.7943	0.7141	0.5742	0.07
	0.495	1.4074	1.1335	0.9363	0.7764	0.6926	0.07
	0.743	1.6190	1.3065	1.0770	0.9077	0.7851	0.07
	0.990	1.8551	1.4909	1.2268	1.0307	0.8898	0.07
	1.237	2.1104	1.6917	1.3901	1.1596	0.9857	0.07
0.1153	0	2.4472	1.6930	1.2708	1.0040	0.8071	0.064
	0.248	2.6966	1.9537	1.4767	1.1571	0.9354	0.064
	0.495	2.9734	2.1823	1.6634	1.3171	1.0595	0.064
	0.743	3.2796	2.4284	1.8653	1.4767	1.2068	0.064
	0.990	3.6075	2.6884	2.0748	1.6489	1.3538	0.064
	1.238	3.9841	2.9741	2.2976	1.8257	1.5001	0.064
0.2811	0	2.8032	1.9725	1.4209	1.1492	0.8919	0.056
	0.248	3.3152	2.3931	1.7905	1.3873	1.1082	0.056
	0.495	3.8372	2.7808	2.0899	1.6214	1.2927	0.056
	0.742	4.4071	3.2030	2.4089	1.8693	1.5035	0.056
	0.990	4.9929	3.6393	2.7420	2.1286	1.6933	0.056
	1.237	5.6341	4.1046	3.0955	2.4011	1.9282	0.056
0.5399	0	2.1427	1.6256	1.2532	0.9935	0.7737	0.043
	0.248	2.8411	2.1421	1.6535	1.3024	1.0426	0.043
	0.495	3.6268	2.7098	2.0746	1.6222	1.2847	0.043
	0.743	4.4324	3.2808	2.4927	1.9356	1.5329	0.043
	0.990	5.4671	4.0188	3.0280	2.3347	1.8471	0.043
	1.238	6.5013	4.7359	3.5413	2.7138	2.1278	0.043
1	0	1.1790	0.9735	0.7540	0.6674	0.5448	0.02
	0.247	1.7935	1.4275	1.1473	0.9294	0.7616	0.02
	0.495	2.5125	1.9593	1.5443	1.2101	0.9834	0.02
	0.743	3.4276	2.6010	2.0098	1.5766	n.a.	0.02
	0.990	4.5425	3.3645	2.5458	1.9682	1.5340	0.02
	1.238	5.7823	4.2008	3.1256	2.3756	1.7959	0.02

Table 4: Results of the thermal conductivity measurements: ethanol mole fraction of the INN-free solvent mixture $\hat{x}_E$, overall INN molality b_{INN}, temperature T, thermal conductivity λ. The pressure is 101.3 kPa. The standard uncertainties are $u(\hat{x}_E) = 0.0005$ mol mol^{-1}, $u(b_{INN}) = 0.005$ mol kg^{-1}, $u(T) = 0.2$ K, $u_r(\lambda) = 0.03$ and $u(p) = 3$ kPa.

| $\hat{x}_E$ | b_{INN} | λ / mW m^{-1}K^{-1} | | |
mol mol^{-1}	mol kg^{-1}	$T = 288.15$ K	298.15 K	308.15 K
0	0	598.3	611.8	632.9
	0.252	509.9	545.4	563.8
	0.497	471.7	519.1	544.6
	0.754	507.0	531.7	555.7
	1.004	498.1	525.1	546.5
0.2811	0	320.7	322.8	327.7
	0.246	313.1	317.8	316.8
	0.500	313.5	311.6	307.5
	0.751	321.3	319.9	312.7
	0.932	302.4	314.4	318.8
1	0	162.9	161.9	159.5
	0.252	173.6	171.4	173.8
	0.501	172.9	184.5	184.2
	0.748	167.1	175.0	184.6
	0.992	154.7	161.9	171.1

Table 5: Results of the heat capacity measurements: ethanol mole fraction of the INN-free solvent mixture $\hat{x}_E$, overall INN molality b_{INN}, temperature T, heat capacity c_p. The pressure is 101.3 kPa. The standard uncertainties are $u(\hat{x}_E) = 0.0005$ mol mol^{-1}, $u(b_{INN}) = 0.005$ mol kg^{-1}, $u(T) = 0.2$ K and $u(p) = 3$ kPa. The relative standard uncertainties of the isobaric heat capacity are given in the table.

$\hat{x}_E$	b_{INN}	c_p / J mol^{-1}K^{-1}			$u_r(c_p)$
mol mol^{-1}	mol kg^{-1}	$T = 288.15$ K	298.15 K	308.15 K	
0	0	75.8	75.6	75.8	0.05
	0.251	71.6	72.2	72.9	0.05
	0.500	72.1	73.6	74.3	0.05
	0.753	70.9	71.0	72.7	0.05
	1.003	70.4	71.1	73.6	0.05
0.2811	0.246	86.7	90.2	95.5	0.1
	0.500	79.9	76.5	86.2	0.1
	0.751	76.1	83.9	87.6	0.1
	0.932	78.5	82.6	85.5	0.1
1	0	111.2	113.2	115.7	0.05
	0.252	103.3	105.3	109.6	0.05
	0.501	97.0	105.1	108.0	0.05
	0.748	89.6	95.6	102.7	0.05
	0.992	80.4	85.8	92.3	0.05

Table 6: Parameters of the correlations for the pure component properties of ethanol and water, cf. Eq. (8).

Property	Component	a	b	c
Molar volume	ethanol	$5.4893 \cdot 10^1$	$-3.8681 \cdot 10^{-2}$	$1.7183 \cdot 10^{-4}$
v / cm³ mol^{-1}	water	$2.3432 \cdot 10^1$	$-4.0429 \cdot 10^{-2}$	$7.5233 \cdot 10^{-5}$
Viscosity	ethanol	$2.2409 \cdot 10^1$	$-1.2232 \cdot 10^{-1}$	$1.7048 \cdot 10^{-4}$
η / mPa s	water	$2.1979 \cdot 10^1$	$-1.2303 \cdot 10^{-1}$	$1.7550 \cdot 10^{-4}$
Thermal conductivity	ethanol	$2.1374 \cdot 10^2$	$-1.7541 \cdot 10^{-1}$	-
λ / mW m^{-1} K^{-1}	water	$1.0047 \cdot 10^2$	$1.7235 \cdot 10^0$	-
Isobaric heat capacity	ethanol	$4.6381 \cdot 10^1$	$2.2467 \cdot 10^{-1}$	-
c_p / J mol^{-1} K^{-1}	water	$7.5733 \cdot 10^1$	-	-

Table 7: Parameters of the correlations for the description of the excess of molar volume, viscosity, thermal conductivity and isobaric heat capacity of the salt-free solvent mixtures, cf. Eqs. (9) - (10).

		A	B	C
Molar volume v / cm³ mol^{-1}	d	$-7.1947 \cdot 10^0$	$2.4990 \cdot 10^0$	-
	e	$9.9041 \cdot 10^{-3}$	$-2.8522 \cdot 10^{-3}$	-
	f	-	-	-
Viscosity η / mPa s	d	$2.0678 \cdot 10^2$	$-4.5683 \cdot 10^2$	$4.6191 \cdot 10^2$
	e	$-1.2205 \cdot 10^0$	$2.7708 \cdot 10^0$	$-2.8238 \cdot 10^0$
	f	$1.8104 \cdot 10^{-3}$	$-4.2196 \cdot 10^{-3}$	$4.3233 \cdot 10^{-3}$
Thermal conductivity λ / mW m^{-1} K^{-1}	d	$3.1291 \cdot 10^2$	$-2.9868 \cdot 10^2$	-
	e	$-3.1908 \cdot 10^0$	$2.5673 \cdot 10^0$	-
	f	-	-	-
Isobaric heat capacity c_p / J mol^{-1}K^{-1}	d	$-5.5381 \cdot 10^1$	$-1.5448 \cdot 10^2$	-
	e	$3.7132 \cdot 10^{-1}$	$3.7778 \cdot 10^{-1}$	-
	f	-	-	-

Table 8: Parameters of the correlations for the description of the influence of INN on the molar volume, viscosity, thermal conductivity and isobaric heat capacity, cf. Eq. (11) - (12).

|		D	E	F	G	H	I	J	K
Molar volume	g	$1.5105 \cdot 10^2$	$3.2334 \cdot 10^2$	$-4.3031 \cdot 10^2$	$8.0516 \cdot 10^1$	$1.2457 \cdot 10^1$	$-9.4439 \cdot 10^2$	$-1.8594 \cdot 10^3$	$3.0156 \cdot 10^3$
v / cm³ mol^{-1}	h	$1.7126 \cdot 10^{-1}$	$-1.1008 \cdot 10^0$	$9.3392 \cdot 10^{-1}$	$4.7319 \cdot 10^{-2}$	$4.7260 \cdot 10^{-1}$	$4.4373 \cdot 10^0$	$4.9317 \cdot 10^0$	$-1.0261 \cdot 10^1$
Viscosity	g	$2.9017 \cdot 10^1$	$-5.1620 \cdot 10^2$	$5.4409 \cdot 10^3$	$-4.7154 \cdot 10^3$	$1.0185 \cdot 10^4$	$4.3117 \cdot 10^4$	$-1.8872 \cdot 10^5$	$1.4078 \cdot 10^5$
η / mPa s	h	$1.8530 \cdot 10^{-2}$	$1.7273 \cdot 10^0$	$-1.7125 \cdot 10^1$	$1.4700 \cdot 10^1$	$-3.2591 \cdot 10^1$	$-1.2897 \cdot 10^2$	$5.8451 \cdot 10^2$	$-4.3872 \cdot 10^2$
Thermal conductivity	g	$-8.8523 \cdot 10^4$	$4.0189 \cdot 10^5$	$-3.2120 \cdot 10^5$	-	$4.2299 \cdot 10^6$	$-1.8809 \cdot 10^7$	$1.4604 \cdot 10^7$	-
λ / mW m^{-1}K^{-1}	h	$2.3937 \cdot 10^2$	$-1.0879 \cdot 10^3$	$8.7986 \cdot 10^2$	-	$-1.1801 \cdot 10^4$	$5.2258 \cdot 10^4$	$-4.0657 \cdot 10^4$	-
Isobaric heat capacity	g	$-4.5294 \cdot 10^3$	$-1.9584 \cdot 10^4$	$1.8072 \cdot 10^4$	-	$7.9355 \cdot 10^4$	$-2.3717 \cdot 10^3$	$-2.6867 \cdot 10^3$	-
c_p / J mol^{-1}K^{-1}	h	$1.3733 \cdot 10^1$	$4.3232 \cdot 10^1$	$-3.8356 \cdot 10^1$	-	$-2.2600 \cdot 10^2$	$5.1300 \cdot 10^2$	$-5.3960 \cdot 10^2$	-
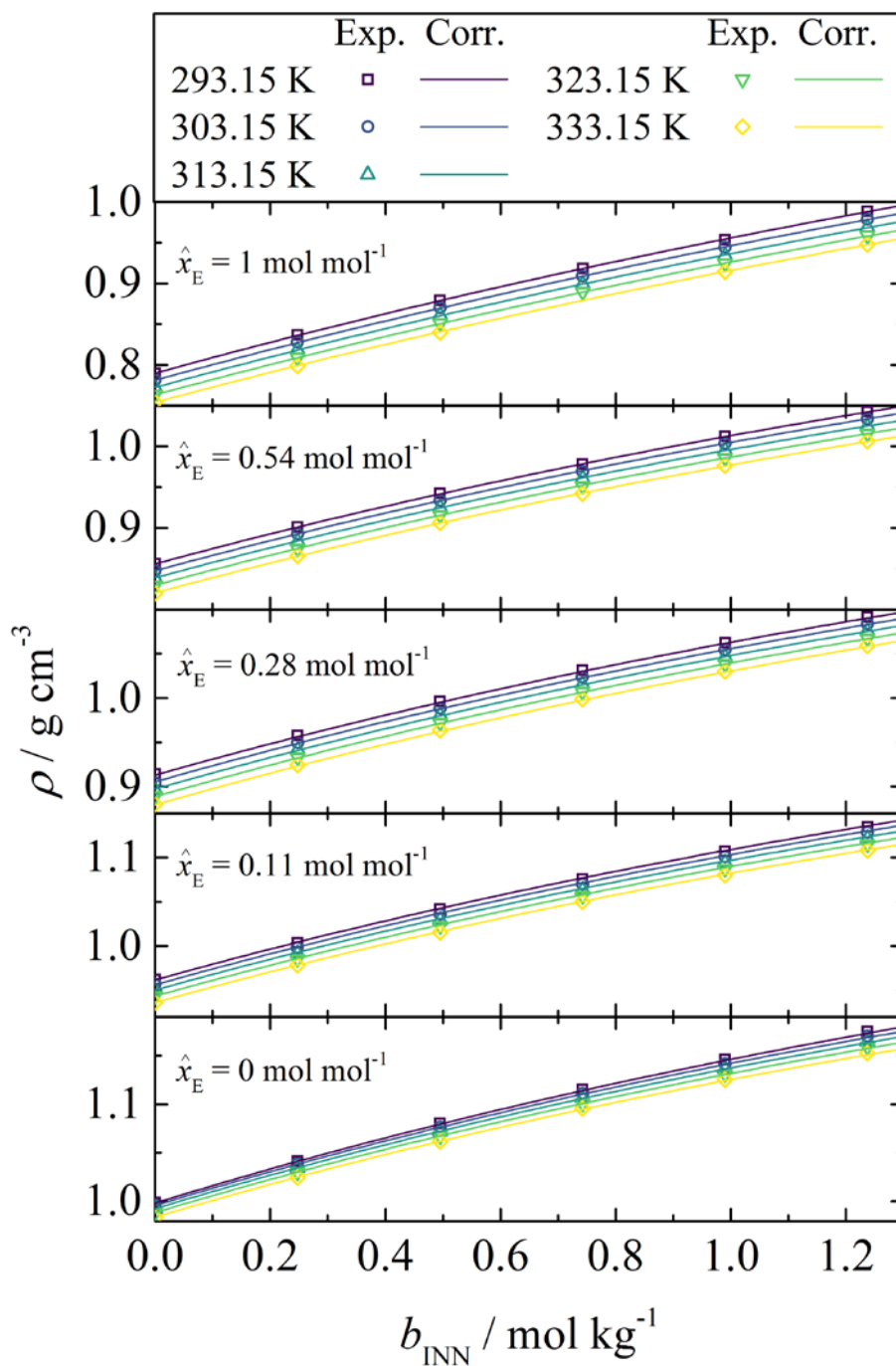
Figure 1: Densities ρ of solutions of INN + ethanol + water at 101.3 kPa. Symbols are experimental results. Experimental uncertainties are always within symbol size. Lines are empirical correlations, cf. Eqs. (5) - (14), with parameters listed in Tables 6 - 8.
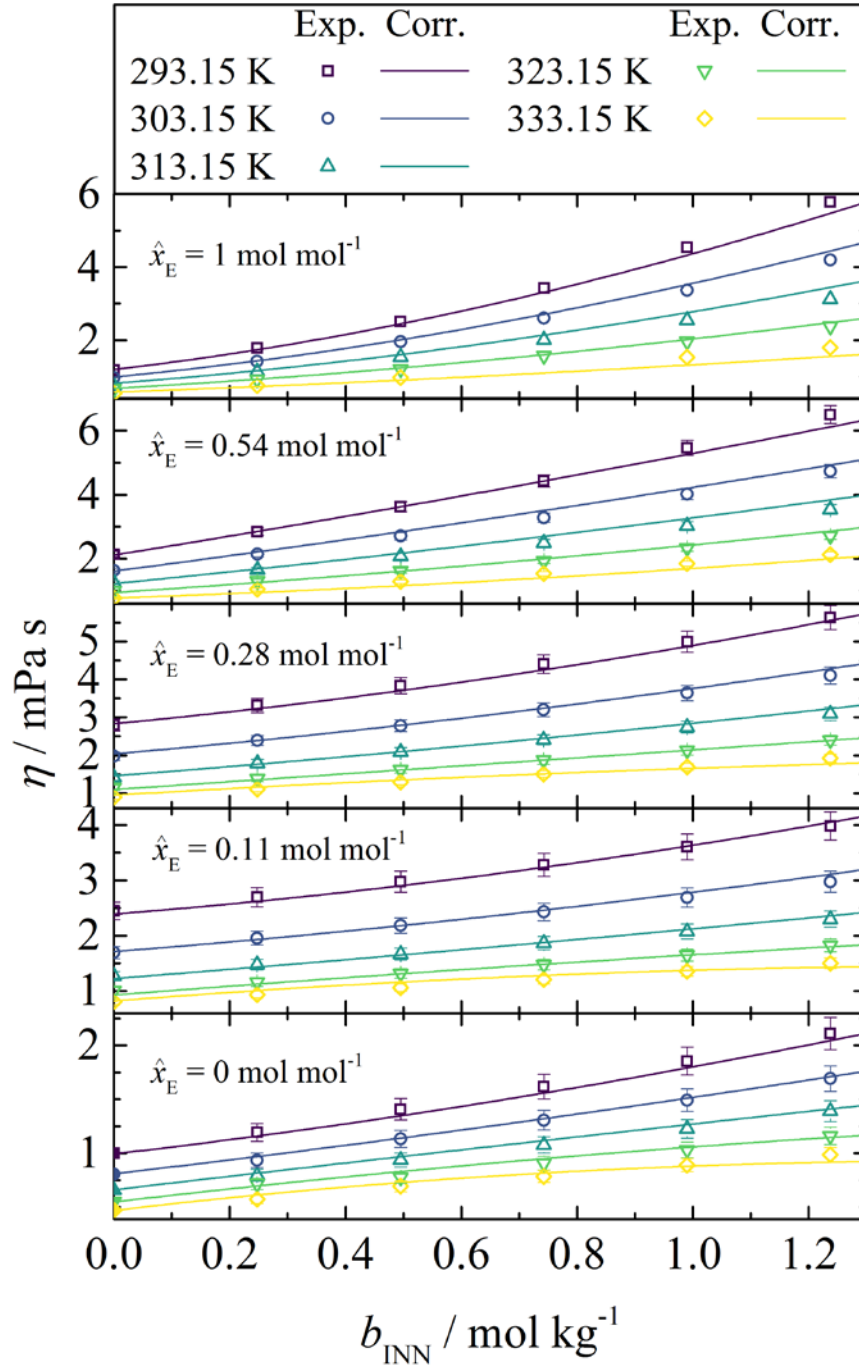
Figure 2: Viscosities η of solutions of INN + ethanol + water at 101.3 kPa. Open symbols are experimental results. Error bars indicate the experimental standard uncertainty. Lines are empirical correlations, cf. Eqs. (6) - (14), with parameters listed in Tables 6 - 8. Solid symbols at $b_{INN} = 0$ mol kg^{-1}, $\hat{x}_E = 0$ mol mol^{-1} are experimental data taken from the literature[42].
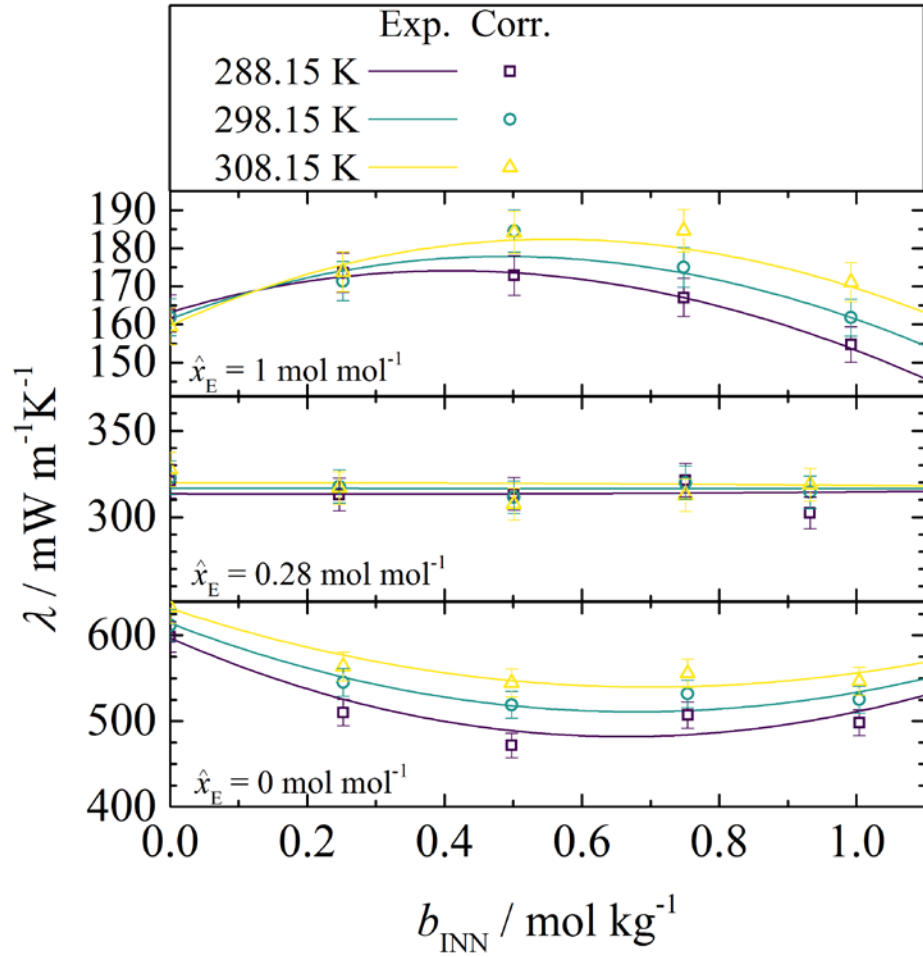
Figure 3: Thermal conductivities λ of solutions of INN + ethanol + water at 101.3 kPa. Symbols are experimental results. Error bars indicate the experimental standard uncertainty. Lines are empirical correlations, cf. Eqs. (6) - (14), with parameters listed in Tables 6 - 8.
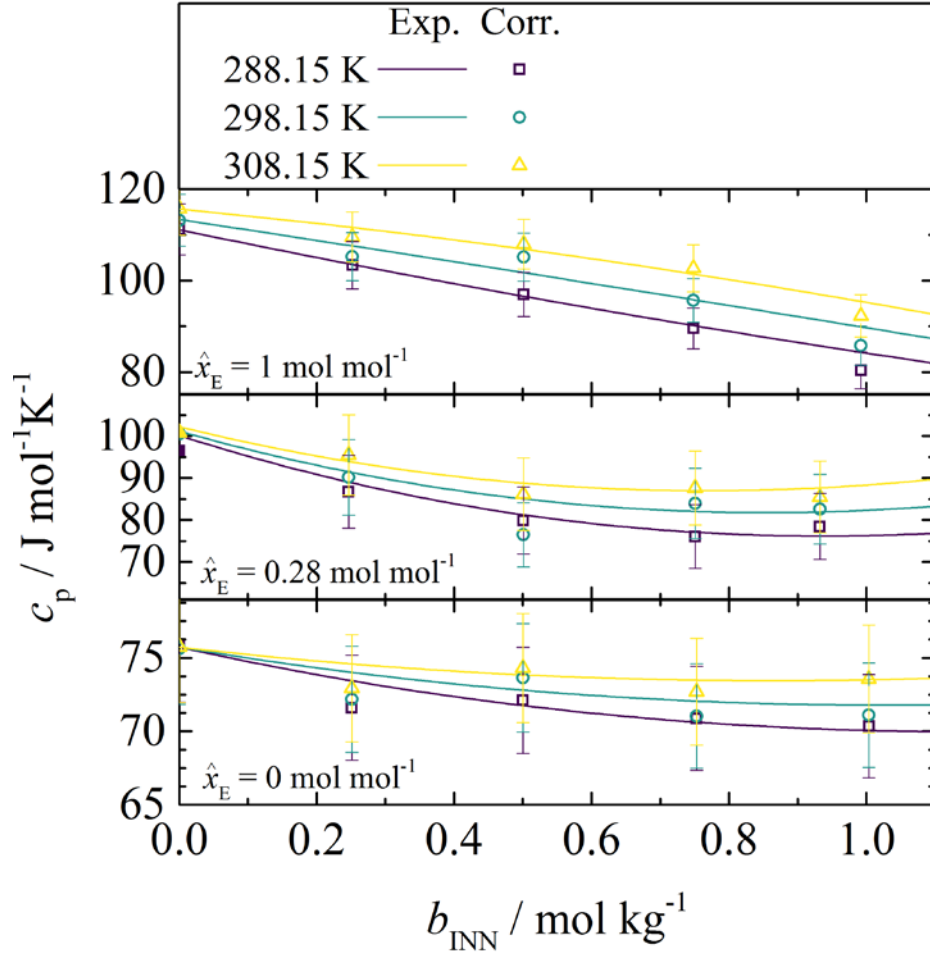
Figure 4: Isobaric heat capacities c_p of solutions of INN + ethanol + water at 101.3 kPa. Open symbols are experimental results. Error bars indicate the experimental standard uncertainty. Lines are empirical correlations, cf. Eqs. (6) - (14), with parameters listed in Tables 6 - 8. Solid symbols at $b_{INN} = 0$ mol kg^{-1}, $\hat{x}_E = 0.28$ mol mol^{-1} are experimental data taken from the literature[39,40].

TOC Graphic